J Fluoresc (2013) 23:425–437
DOI 10.1007/s10895-013-1156-3

ORIGINAL PAPER

N-Triazinyl Derivatives of 1- and 9-aminoanthracene: Synthesis and Photo-Physical Properties

Hana Přichystalová · Numan Almonasy · Miloš Nepraš · Filip Bureš · Miroslav Dvořák · Martin Michl · Jiři Čermák · Ladislav Burgert

Received: 20 June 2012 / Accepted: 7 January 2013 / Published online: 18 January 2013

Abstract New *N*-triazinyl derivatives were synthesized by reaction of cyanuric chloride with 1- and 9-aminoanthracenes and subsequent nucleophilic substitution of chlorine atoms on triazinyl ring with methoxy and/or phenylamino groups. The compounds were characterized by ^{1}H and ^{13}C NMR and mass spectra. The influence of the chemical structure and solvent polarity on the UV/Vis absorption and fluorescence spectra and fluorescence quantum yields were investigated. Semi-empirical computations revealed highly polar CT states in singlet excited state manifold connected with charge-transfer from the hydrocarbon moiety to the triazinyl ring. The relationships between the CT-to-emitting state energy gap, solvent polarity and fluorescence quantum yield were discussed.

Keywords *N*-Triazinyl aminoanthracenes · Synthesis · Fluorescence spectra · Quantum yield · Quenching

H. Přichystalová · N. Almonasy (✉) · M. Nepraš · F. Bureš · L. Burgert
Institute of Organic Chemistry and Technology and Institute of Polymeric Materials, Faculty of Chemical Technology, University of Pardubice, Studentská 573, Pardubice CZ-532 10, Czech Republic
e-mail: numan.almonasy@upce.cz

M. Dvořák · M. Michl
Department of Physical Electronics, Faculty of Nuclear Sciences and Physical Engineering, Czech Technical University in Prague, v Holešovičkách 2, Prague CZ-180 00, Czech Republic

J. Čermák
Research Institute for Organic Syntheses, Rybitví 296, Pardubice CZ-533 54, Czech Republic

Introduction

In a molecular bichromophoric system with different chromophores mutually connected by a molecular unit, the excitation may occur in one chromophore and then be transferred to another one. This process is known as the electronic (or excitation) energy transfer (EET) [1]. The essential condition for efficient EET is the strong overlap between the donor emission and acceptor absorption spectra. The phenomenon of EET plays nowadays very important role in light-induced processes in biology, biochemistry and in technical applications (e.g. materials for optoelectronics) [2, 3].

During the past decade, we have been interested in the synthesis and study of photo-physical properties of bichromophoric systems consisting of aromatic polycyclic amines and triazinyl ring as the bridge [4, 5]. In order to understand the characteristics of EET in such compounds, the detailed knowledge of photo-physical behaviour of the individual chromophore subsystems is necessary. Particularly, for the through-bond mechanism of EET, the strength of electronic coupling between the chromophor and the bridge moieties is of great importance. Earlier we published the synthesis and photo-physical characteristics, including solvent polarity effects, of *N*-triazinyl derivatives of 3-aminobenzanthrone [6], 1- and 2-aminopyrenes [7], 3-aminoperylene [8] and 2-aminoanthracene [9]. The most remarkable feature of all investigated *N*-triazinyl derivatives (except the derivatives of 2-aminopyrene [7]) is the dramatic influence of the number of chlorine atoms and the solvent polarity on the fluorescence quantum yield. The compounds containing one or two chlorine atoms on the triazinyl ring have good potentiality for their using as fluorescent labels. The advantage of these labels is they are non-fluorescent and only after the linking to a substrate, the effects of their fluorescence

properties appear. They will be used also as the intermediates for the preparation of ne bichromophoric systems.

Recently, using semi-empirical AM1, CNDO/S and ZINDO/S methods, we have calculated the excited state characteristics of *N*-triazinyl derivatives of 1-aminopyrene [10]. Besides the L_a and L_b transitions localized on aminopyrene moiety, the excited states connected with the CT from aminopyrene to the triazinyl ring were found. The energy of such strongly polar CT states depends on the substituents on triazinyl ring and on solvent polarity. The relationships between the CT-to-emitting state energy gap, solvent polarity and fluorescence quantum yield of the studied compounds were discussed.

To confirm the common validity of the role of the CT states on the q_F of*N*-triazinyl derivatives of aromatic polynuclear amines, we report herein the synthesis of new *N*-triazinyl derivatives of 1- and 9-aminoanthracenes. Calculated geometries (AM1) and excited state characteristics (ZINDO/S) for 1-, 2- and 9-aminoanthracene derivatives are presented and discussed.

Materials and Methods

1-Aminoanthracene (**1-AA**), cyanuric chloride, aniline, methanol and other solvents for the syntheses were used as received without further purification. 9-Aminoanthracene (**9-AA**) and *N*-acetyl derivatives of 1- and 9-aminoanthracene were prepared according literature procedures [11-13]. The course of the reactions and purity of the substances were checked by TLC, HPLC, and by comparison of fluorescence excitation spectra with absorption spectra of the final products. The melting points of the synthesized compounds were determined on a Buchi 510 melting point apparatus.

The samples for absorption spectra and fluorescence measurements were prepared by preparative TLC on Silufol UV 254 plates. All the solvents used were of spectroscopic grade and were checked for their own fluorescence.

The absorption spectra were measured on a UV/Vis Perkin-Elmer Lambda 35 spectrophotometer at room temperature. The steady-state fluorescence spectra were measured on a Perkin-Elmer LS 55 spectrophotometer. The instrument provides corrected excitation spectra directly; the fluorescence spectra were corrected for the characteristics of the emission monochromator and for the photomultiplier response. For fluorescence measurements, the solutions of very low concentration about 10^{-6}mol/L (optical density~0.05 at the excitation wavelength in 1-cm cell) were used.

The fluorescence quantum yields were measured using quinine sulphate (q_F=0.54 in 0.5 mol/L H_2SO_4) [14] as the standard. Deaeration of the samples by bubbling with N_2 did not change the spectra and q_F.

The fluorescence kinetics measurements were performed on an Edinburgh Analytical Instruments FS/FL spectrophotometer that employs time-correlated single photon counting (TCSPC) detection. Pulse IBH Nanoled-03 (370 nm) diode was used as the excitation source to excite the set of studied compounds near the centre of the absorption band. Instrument response function FWHM was <1.5 ns. The fluorescence signal was recorded at 450 nm at the maximum of the fluorescence band. The fluorescence lifetimes were obtained by multiexponential deconvolution fitting procedure.

The chemical structures were confirmed by MS, ^{1}H and ^{13}C NMR spectra and elemental analysis.^{1}H and ^{13}C NMR spectra were recorded at 400 and 100 MHz respectively, with a Bruker AVANCE 400 instrument at 25 °C. Chemical shifts are reported in ppm relative to the signal of Me_4Si. The residual solvent signal in the ^{1}H and ^{13}C NMR spectra was used as an internal reference (DMSO-d_6–2.55 and 39.51 ppm). Apparent resonance multiplicities are described as s (singlet), br s (broad singlet), d (doublet) and m (multiplet). Some target compounds showed two sets of signals or broad signals in ^{1}H and ^{13}C NMR spectra (DMSO-d_6) as a result of acidic hydrogen scrambling (NH), tautomerism or possible association similar to that we have recently observed for imidazoles [15]. This effect was most encountered for methoxy substituted derivatives and could be partially suppressed by using diluted samples.

Mass spectra were acquired on a LC/MS system LC-MSD TRAP XCT Plus (Agilent Technologies, USA) using direct infusion measurement. Negative and positive-ion APCI mass spectra were recorded in mass range 50–1,500 Da. The ion trap analyzer was tuned to obtain an optimal response in the range of expected m/z values. Other APCI ion source parameters were as follows: a drying gas flow of 7 l.min^{-1}, a nebulizer gas pressure of 60 psi and drying gas temperature 350 °C. The samples were dissolved in acetonitrile (MeCN) for HPLC (Sigma-Aldrich) at appropriate concentrations for MS identification.

Experimental

The synthesis of target compounds is shown in Scheme 1.

General Procedure for the Synthesis of N-(4,6-dichloro-1,3,5-triazin-1-yl)-1-aminoanthracene and N-(4,6-dichloro-1,3,5-triazin-9-yl)-9-aminoanthracene

Cyanuric chlorid (5 g, 27 mmol) was dissolved in 100 mL of acetone and sodium carbonate was added and the mixture was cooled to −5 to 0 ° C. The solution of amine (5 g, 26 mmol) in 100 mL of acetone was added dropwise (the reaction with 9-aminoanthracene was carried out under nitrogen atmosphere). The temperature of the reaction mixture was maintained between −5 to 10 °C and the reaction was continuously monitored

Scheme 1 Synthetic scheme of the target compounds

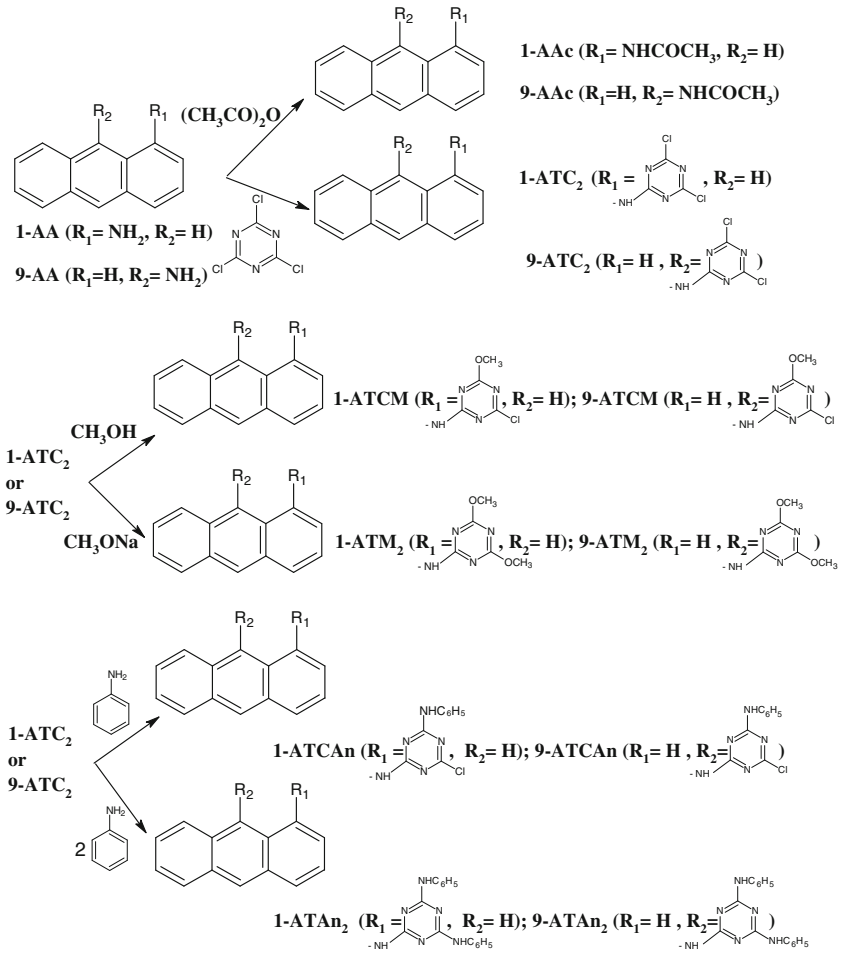

by TLC. After 4 h the reaction mixture was poured into water (100 mL) and the precipitated crude product was filtered off and dried. The crude product was recrystallized from toluene.

N-(4,6-Dichloro-1,3,5-triazin-1-yl)-1-aminoanthracene (1-ATC$_2$)

Obtained 8.3 g (57 %) as a brown solid; mp>300 °C. ^{1}H NMR (DMSO-d_6, 400 MHz): δ=7.59–7.65 (m, 4H, **1-AA**), 8.15–8.20 (m, 3H, **1-AA**), 8.69 (s, 1H, **1-AA**), 8.73 (s, 1H, **1-AA**), 11.36 (br s, 1H, NH). ^{13}C NMR (DMSO-d_6, 100 MHz): δ=121.75, 123.34, 124.96, 126.08, 126.12, 126.72, 127.25, 127.86, 127.91, 128.49, 131.31, 131.32, 131.77, 131.97, 164.62, 166.02. MS: (APCI$^+$): m/z 341 [M+H]$^+$ (M.W. 340 g/mol). EA: calculated for $C_{17}H_{10}Cl_2N_4$: C 59.84 %, H 2.95 %, Cl 20.78 %, N 16.42 %; found: C 59.52 %, H 3.28 %, Cl 20.87 %, N 16.33 %.

N-(4,6-Dichloro-1,3,5-triazin-9-yl)-9-aminoanthracene (9-ATC$_2$)

Obtained 4.2 g (48 %) as a yellow-green solid; mp 296–299 °C. ^{1}H NMR (DMSO-d_6, 400 MHz): δ=7.61–7.65 (m, 4H, **9-AA**), 8.10–8.12 (m, 2H, **9-AA**), 8.21–8.24 (m, 2H, **9-AA**), 8.76 (s, 1H, **9-AA**), 11.53 (br s, 1H, NH). ^{13}C NMR (DMSO-d_6, 100 MHz): δ=123.35, 125.81, 126.86, 127.73, 128.23, 128.60, 128.92, 131.29, 166.58, 169.29. MS: (APCI$^+$): m/z 341 [M+H]$^+$ (M.W. 340 g/mol). EA: calculated for $C_{17}H_{10}Cl_2N_4$: C 59.84 %, H 2.95 %, Cl 20.78 %, N 16.42 %; found: C 59.70 %, H 3.13 %, Cl 20.89 %, N 16.28 %.

General Procedure for the Synthesis of N-(4-chloro-6-methoxy-1,3,5-triazin-1-yl)-1-aminoanthracene and N-(4-chloro-6-methoxy-1,3,5-triazin-9-yl)-9-aminoanthracene

A solution of **ATC$_2$** (0.5 g, 1.5 mmol) in 15 mL methanol and dried sodium carbonate (0.15 g, 1.4 mmol) was stirred under nitrogen atmosphere at 25 °C for 2 h. TLC (cyclohexane-ethyl acetate 3:1) was used to monitor progress of the reaction and after complete disappearance of starting material, the reaction was poured into water (100 mL) and the precipitate was filtered off and dried. The crude product was purified by recrystalization from toluene and by subsequent column chromatography on silica gel (cyclohexane-ethyl acetate 3:1).

N-(4-Chloro-6-methoxy-1,3,5-triazin-1-yl)-1-aminoanthracene (1-ATCM)

Obtained 0.42 g (85 %) as a light brown solid; mp 205–208 °C. ^{1}H NMR (DMSO-d_6, 400 MHz): δ=3.75+4.00 (2×s, 3H, OMe), 7.56–7.70 (m, 4H, **1-AA**), 8.10–8.19 (m, 3H, **1-AA**), 8.70 (s, 2H, **1-AA**), 10.81 (br s, 1H, NH). ^{13}C NMR (DMSO-d_6, 100 MHz): δ=55.07 (br), 121.82, 125.03, 125.98, 126.04, 126.11, 126.61, 127.05, 127.89, 128.54, 131.19, 131.26, 131.86, 132.72, 134.70, 170.49, 170.94. MS: (APCI$^+$): m/z 337 [M+H]$^+$ (M.W. 336 g/mol). EA: calculated for $C_{18}H_{13}ClN_4O$: C 64.19 %, H 3.89 %, Cl 10.53 %, N 16.64 %, O 4.75 %; found: C 63.87 %, H 4.03 %, Cl 10.84 %, N 16.45 %, O 4.81 %.

N-(4-chloro-6-methoxy-1,3,5-triazin-9-yl)-9-aminoanthracene (9-ATCM)

Obtained 0.41 g (84 %) as a yellow solid; mp 218–221 °C. ^{1}H NMR (DMSO-d_6, 400 MHz): δ=3.52+4.10 (2×s, 3H, OMe), 7.58–7.64 (m, 4H, **9-AA**), 8.06–8.07 (m, 2H, **9-AA**), 8.20–8.24 (m, 2H, **9-AA**), 8.72+8.74 (2×s, 1H, **9-AA**), 10.91+10.98 (2×br s, 1H, NH). ^{13}C NMR (DMSO-d_6, 100 MHz): δ=54.78+55.34, 123.40+123.57, 126.50+126.67, 126.60+126.70, 127.90+128.17, 128.18+128.24, 128.56+128.58, 131.31+131.37, 167.63+167.80, 169.95+170.44, 170.85+170.94. MS: (APCI$^+$): m/z 337 [M+H]$^+$ (M.W. 336 g/mol). EA: calculated for $C_{18}H_{13}ClN_4O$: C 64.19 %, H 3.89 %, Cl 10.53 %, N 16.64 %, O 4.75 %; found: C 64.18 %, H 4.02 %, Cl 10.75 %, N 16.51 %, O 4.54 %.

General Procedure for the Synthesis of N-(4,6-dimethoxy-1,3,5-triazin-1-yl)-1-aminoanthracene and N-(4,6-dimethoxy-1,3,5-triazin-9-yl)-9-aminoanthracene

A 50 mL Erlenmeyer flask equipped with an electromagnetic stirrer was charged with ATC_2 (0.5 g, 1.5 mmol) and 0.2 g (3.7 mmol) of sodium methanolate in 15 mL methanol. The reaction was refluxed for 2 h, cooled to 25 °C and the precipitate was filtered off. Diluting the mother liquor with water delivered a second portion of product. By recrystallization of the combined products (cyclohexane-ethyl acetate 1:1) afforded pure products.

N-(4,6-Dimethoxy-1,3,5-triazin-1-yl)-1-aminoanthracene ($1\text{-}ATM_2$)

Obtained 0.34 g (69 %) as a brown solid; mp. 200–210 °C. ^{1}H NMR (DMSO-d_6, 400 MHz): δ=3.87 (br s, 6H, 2×OMe), 7.54–7.60 (m, 3H, **1-AA**), 7.69 (d, 1H, J=6.8 Hz, **1-AA**), 8.05 (d, 1H, J=8.8 Hz, **1-AA**), 8.13–8.17 (m, 2H, **1-AA**), 8.67 (s, 1H, **1-AA**), 8.70 (s, 1H, **1-AA**), 10.26 (br s, 1H, NH). ^{13}C NMR (DMSO-d_6, 100 MHz): δ=54.35, 121.93, 122.55, 125.18, 125.85, 125.94, 126.30, 126.46, 127.64, 127.86, 128.56, 131.03, 131.17, 131.95, 133.62, 168.05, 172.17. MS: (APCI$^+$): m/z 333 [M+H]$^+$ (M.W. 332 g/mol). EA: calculated for $C_{19}H_{16}N_4O_2$: C 68.66 %, H 4.85 %, N 16.86 %, O 9.63 %; found: C 68.55 %, H 4.99 %, N 16.72 %, O 9,74 %.

N-(4,6-Dimethoxy-1,3,5-triazin-9-yl)-9-aminoanthracene ($9\text{-}ATM_2$)

Obtained 0.32 g (65 %) as a light brown solid; mp 205–208 °C. ^{1}H NMR (DMSO-d_6, 400 MHz): δ=3.50 (s, 3H, OMe), 4.06 (s, 3H, OMe), 7.56–7.61 (m, 4H, **9-AA**), 8.05–8.06 (m, 2H, **9-AA**), 8.18–8.21 (m, 2H, **9-AA**), 8.68 (s, 1H, **9-AA**), 10.36 (br s, 1H, NH). ^{13}C NMR (DMSO-d_6, 100 MHz): δ=53.84, 54.47, 123.73, 125.51, 126.01, 126.15, 128.34, 128.43, 129.35, 131.35, 168.84, 172.12. MS: (APCI$^+$): m/z 333 [M+H]$^+$ (M.W. 332 g/mol). EA: calculated for $C_{19}H_{16}N_4O_2$: C 68.66 %, H 4.85 %, N 16.86 %, O 9.63 %; found: C 68.72 %, H 5.01 %, N 16.88 %, O 9.39.

General Procedure for the Synthesis of N-(4-chloro-6-phenylamino-1,3,5-triazin-1-yl)-1-aminoanthracene N-(4-chloro-6-phenylamino-1,3,5-triazin-9-yl)-9-aminoanthracene

A solution of **ATC_2** (0.2 g, 0.59 mmol) in 20 mL of butanone was cooled to 5–10 °C. Aniline (0.6 mL, 6.6 mmol) and catalytic amount of sodium carbonate were added. The reaction mixture was stirred at 10 °C for 3 h, sodium carbonate was removed by filtration and the mother liquid was poured into cyclohexane (50 mL). The precipitate was filtered off and dried.

N-(4-Chloro-6-phenylamino-1,3,5-triazin-1-yl)-1-aminoanthracene (1-ATCAn)

Obtained 0.19 g (83 %) as a brown solid; mp 265–270 °C. ^{1}H NMR (DMSO-d_6, 400 MHz): δ=7.18–7.36 (m, 3H, Ph), 7.49–7.67 (m, 6H, Ph+**1-AA**), 8.10–8.19 (m, 3H, **1-AA**), 8.71 (s, 2H, **1-AA**), 10.18 (br s, 1H, NH), 10.52 (br s, 1H, NH). ^{13}C NMR (DMSO-d_6, 100 MHz): δ=122.05, 122.30, 123.10, 124.97, 125.91, 125.98, 126.56, 126.82, 127.86, 128.31, 128.59, 129.72, 131.18, 131.25, 131.97, 133.49, 138.43, 139.52, 163.56, 166.03, 168.39. MS: (APCI$^+$): m/z 398 [M+H]$^+$ (M.W. 397 g/mol).

EA: calculated for $C_{23}H_{16}ClN_5$: C 69.43 %, H 4.05 %, Cl 8.91 %, N 17.60 %; found: C 69.12 %, H 4.26 %, Cl 9.08 %, N 17.54 %.

N-(4-Chloro-6-phenylamino-1,3,5-triazin-9-yl)-9-aminoanthracene (9-ATCAn)

Obtained 0.18 g (79 %) as a light brown solid; mp 261–263 °C. ^{1}H NMR (DMSO-d_6, 400 MHz): δ=6.57–6.68 (m,

3H, Ph), 7.05–7.47 (m, 2H, Ph), 7.59–7.62 (m, 4H, **9-AA**), 8.13–8.17 (m, 2H, **9-AA**), 8.20–8.26 (m, 2H, **9-AA**), 8.72 (s, 1H, **9-AA**), 10.09 (br s, 1H, NH), 10.82 (br s, 1H, NH). ^{13}C NMR (DMSO-d_6, 100 MHz): δ=119.32, 123.68+ 123.80, 125.62+125.69, 126.04, 126.39+126.49, 127.73, 128.00, 128.54, 128.73, 129.27, 131.44, 138.07, 163.28, 166.59, 168.50. MS: (APCI$^+$): m/z 398 $[M+H]^+$ (M.W. 397 g/mol). EA: calculated for $C_{23}H_{16}ClN_5$: C 69.43 %, H 4.05 %, Cl 8.91 %, N 17.60 %; found: C 69.34 %, H 4.22 %, Cl 9.07 %, N 17.37 %.

General Procedure for the Synthesis of N-(4,6-phenylamino-1,3,5-triazin-1-yl)-1-aminoanthracene and N-(4,6-diphenylamino-1,3,5-triazin-9-yl)-9-aminoanthracene

A solution of ATC_2 (0.2 g, 0.59 mmol) and aniline (2 mL, 22 mmol) in 20 mL of butanone containing catalytic amounts of sodium carbonate was refluxed with stirring for 2 h. The mixture was filtered to remove the sodium carbonate while hot, the solvent was removed in vacuum and the crude product was recrystallized and subsequently purified by column chromatography on silica gel.

N-(4,6-Diphenylamino-1,3,5-triazin-1-yl)-1-aminoanthracene (1-$ATAn_2$)

Obtained 0.14 g (53 %) as a light brown solid; mp 301–304 °C. ^{1}H NMR (DMSO-d_6, 400 MHz): δ=6.90–6.98 (m, 2H, Ph), 7.09–7.37 (m, 5H, Ph), 7.51–7.58 (m, 3H, Ph), 7.70–7.83 (m, 4H, **1-AA**), 8.05 (d, 1H, J=8.6 Hz, **1-AA**), 8.16 (t, 2H, J=9.6 Hz, **1-AA**), 8.68 (s, 1H, **1-AA**), 8.78 (s, 1H, **1-AA**), 9.31 (br s, 2H, NH), 9.55 (br s, 1H, NH). ^{13}C NMR (DMSO-d_6, 100 MHz): δ=120.09, 121.83, 122.18, 122.95, 125.25, 125.70, 125.80, 126.36, 127.84, 128.22, 128.37, 128.57, 129.40, 131.00, 131.17, 132.13, 134.74, 139.96, 164.04, 165.82. MS: (APCI$^+$): m/z 455 $[M+H]^+$ (M.W. 454 g/mol). EA: calculated for $C_{29}H_{22}N_6$: C 76.63 %, H 4.88 %, N 18.49 %; found: C 76.71 %, H 5.02 %, N 18.27 %.

N-(4,6-Diphenylaamino-1,3,5-triazin-9-yl)-9-aminoanthracene (9-$ATAn_2$)

Obtained 0.14 g (51 %) as a light brown solid; m p 266–270 °C. ^{1}H NMR (DMSO-d_6, 400 MHz): δ=6.57–6.88 (m, 3H, Ph), 7.01–7.16 (m, 2H, Ph), 7.30–7.47 (m, 3H, Ph), 7.51–7.72 (m, 4H, **9-AA**), 7.90–8.08 (m, 2H, Ph), 8.13–8.35 (m, 4H, **9-AA**), 8.66 (s, 1H, **9-AA**), 8.97 (br s, 1H, NH), 9.38 (br s, 1H, NH), 9.64 (br s, 1H, NH). ^{13}C NMR (DMSO-d_6, 100 MHz): δ=120.26, 121.87, 124.30, 125.51, 125.94, 127.77, 128.38, 128.43, 129.00, 130.91, 131.61, 139.70+140.30, 164.49, 166.91. MS: (APCI$^+$): m/z 455 $[M+H]^+$ (M.W. 454 g/mol). EA: calculated for $C_{29}H_{22}N_6$: C 76.63 %, H 4.88 %, N 18.49 %; found: C 76.75 %, H 4.74 %, N 18.51 %.

Results and Discussion

Synthesis

Synthesis of *N*-triazinyl derivatives of polycyclic aromatic amines is the subject of our studies for several years. Generally, these compounds are prepared by the reaction of cyanuric chloride with amines. The two remaining chlorine atoms on the triazine ring are either at once or gradually substituted by electron donating groups (methoxy or fenylamino group). The reaction takes place mainly in acetone in the presence of a weak base ($NaCO_3$ or $NaHCO_3$). In order to achieve the highest selectivity, the general conditions needed to be optimized for every starting amine.

In our previous works we have used 3-aminobenzanthrone [6], 1- and 2-aminopyrenes [7], 3-aminoperylene [8], and 2-aminoanthracene [9] as starting materials. In this study,1- and 9-aminoanthracenes were used as starting material. In comparison with the other amines used, the aminoanthracenes are more reactive and less stable. The reaction of 1-aminoanthracene with cyanuric chloride afforded selectively **ATC_2** at about −5 °C. As expected, the increased temperature led to the reaction of two molecules of amine to yield **ATC_2** and **A_2TC** (2,4-(1-anthracenylamino)-6-chloro-1,3,5-triazine) derivatives. The products remained soluble in the reaction mixture even after dilution with water; so they were precipitated by adding NaCl to the reaction mixture. Relatively pure products were obtained in this way. Due to the relatively rapid oxidation of 9-aminoantracene to anthraquinone, its reaction with cyanuric chloride were performed under the atmosphere of nitrogen or argon. Although the reaction was performed at temperature around −5 °C as in preparation of **1-ATC_2**, both the **9-ATC_2** and **9-A_2TC** (2,4-(9-anthracenylamino)-6-chloro-1,3,5-triazine) compounds were obtained (NMR, MS). The product was precipitated by diluting the reaction mixture with water. The samples for analysis were separated by column chromatography.

For preparation of **ATCM** and **ATCAn**, several experiments at different temperatures were performed, but under all conditions the substitution of one and/or both chlorine atoms on triazinyl ring by electron donating groups occurred and mixtures of **ATCM** and **ATM_2** or **ATCAn** and **$ATAn_2$** were formed. It was practically impossible to obtain these substances in pure form by recrystallization. However, a separation of both substances by column chromatography was successful.

The synthesis of **ATM_2** and **$ATAn_2$** was carried out by the reaction of sodium methanolate or aniline with **ATC_2**. The only impurity, observed on TLC and confirmed by

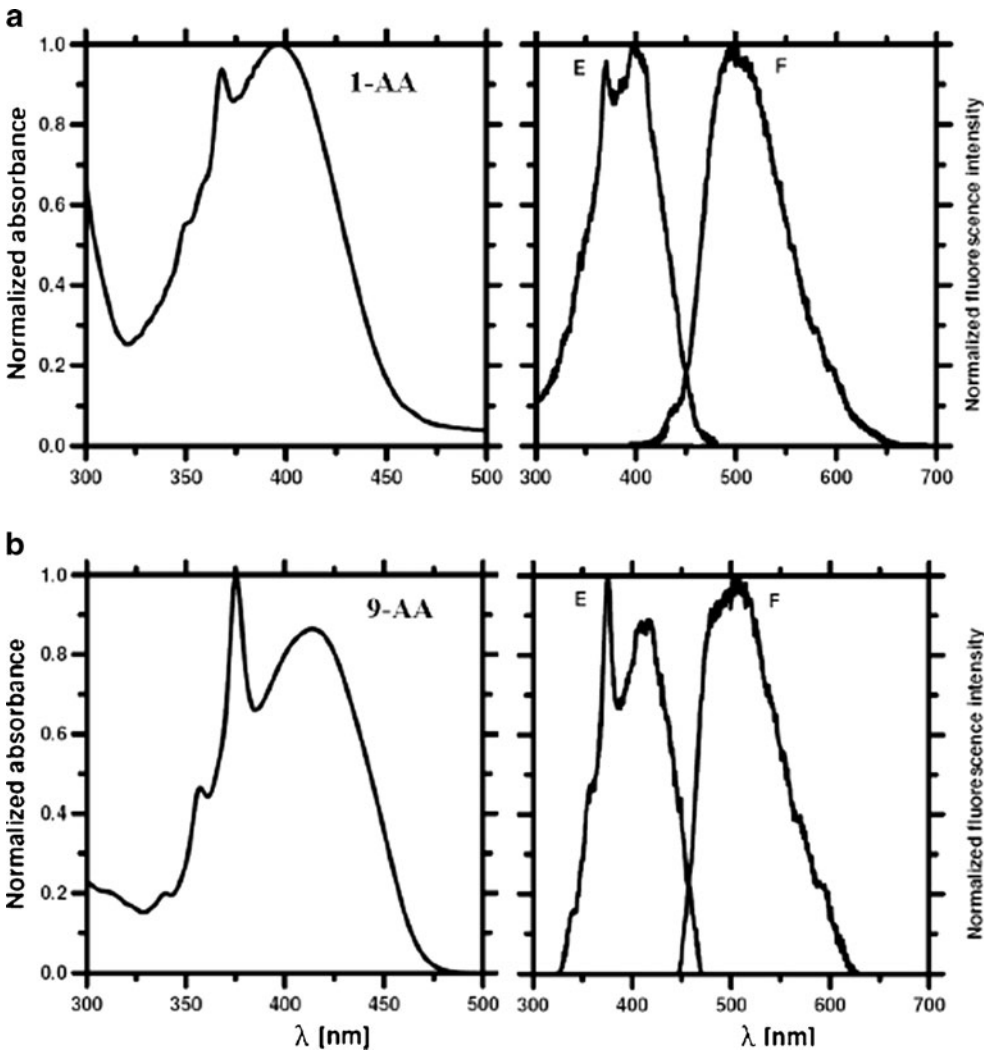

Fig. 1 Absorption (A), excitation (E) and fluorescence (F) spectra of **1-AA** (**a**) and **9-AA** (**b**) in dibutyl ether

Table 1 Absorption (λ_A) and fluorescence (λ_F) maxima (nm) of 1-aminoanthracene derivatives

Comp.	Dibutyl ether		Ethyl acetate		Acetonitrile	
	λ_{A*}	λ_F	λ_{A*}	λ_F	λ_{A*}	λ_F
1-AA	397	498	398	524	390	537
1-AAc	375	409 429	373	416 429	370	430
1-ATC_2	381	–	380	–	381	–
1-ATCM	380	407 430	379	410 430	381	–
1-ATM_2	380	413 435	379	418 434	380	435
1-ATCAn	381	412 435	380	417 434	381	431
1-$ATAn_2$	382	426	382	441	381	450

λ_A^* corresponds to the maximum of the most intensive vibronic band

- no fluorescence was detected

Table 2 Absorption (λ_A) and fluorescence (λ_F) maxima (nm) of 9-aminoanthracene derivatives

Compound	Dibutyl ether		Ethyl acetate		Acetonitrile	
	λ_{A*}	λ_F	λ_{A*}	λ_F	λ_{A*}	λ_F
9-AA	413	507	418	518	414	515
9-AAc	385	403 418	384	403 419	383	401 418
9-ATC_2	385	–	386	–	385	–
9-ATCM	385	403 418	385		385	–
9-ATM_2	385	409 426	385	415	385	415
9-ATCAn	386	411 425	386	421	386	417
9-$ATAn_2$	386	424	386	426	387	427

λ_A^* corresponds to the maximum of the first long-wavelength vibronic band

- no fluorescence was detected

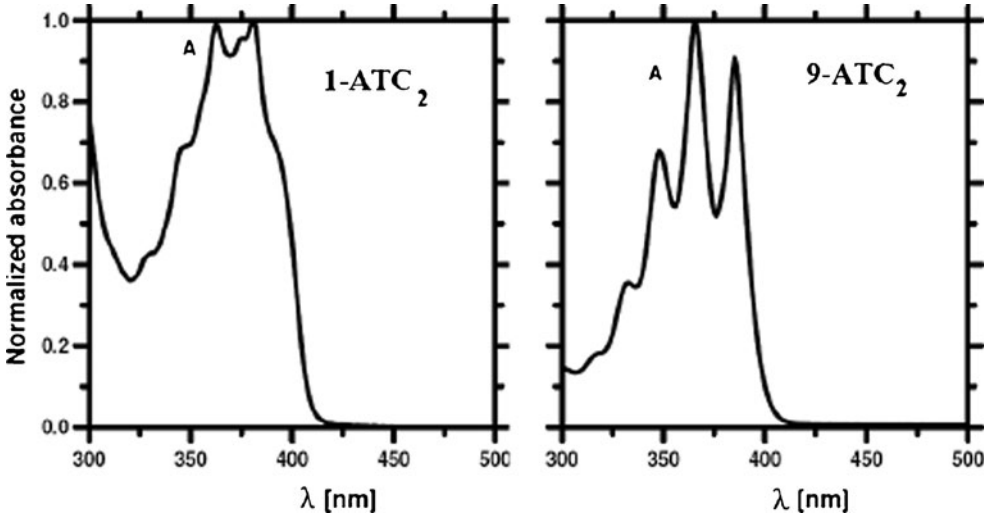

Fig. 2 Absorption spectra of **1-ATC$_2$** and **9-ATC$_2$** in dibutyl ether

NMR and MS analysis, was the **ATCM** and **ATCAn**, respectively. However, only traces of these side products were detected and after recrystallization from toluene the pure products were obtained.

Absorption and Fluorescence Spectra

The absorption spectra of **1-AA** and **9-AA** in the region 300–500 nm are formed by two partially overlapped bands (Fig. 1). The substitution of amino hydrogen atom of the studied amines by electron-withdrawing acetyl group or triazinyl ring causes a strong decrease of a conjugation of amino $2p_\pi$ electrons with anthracene ring. Consequently, the absorption spectra of *N*-acetyl and *N*-triazinyl derivatives resemble more (9-derivatives) or less the spectra of inductively perturbed anthracene derivatives.

The shape of absorption spectra and position of absorption maxima of *N*-triazinyl derivatives of both studied aminoanthracenes are practically not influenced either by the triazinyl substituents or the solvent polarity (Tables 1 and 2, Figs. 2 and 3).

In contrast to the absorption spectra, the fluorescence spectra of both studied aminoanthracenes exhibit a broad band without or only with a hint of vibronic structure. Increasing solvent polarity by going from dibutyl ether

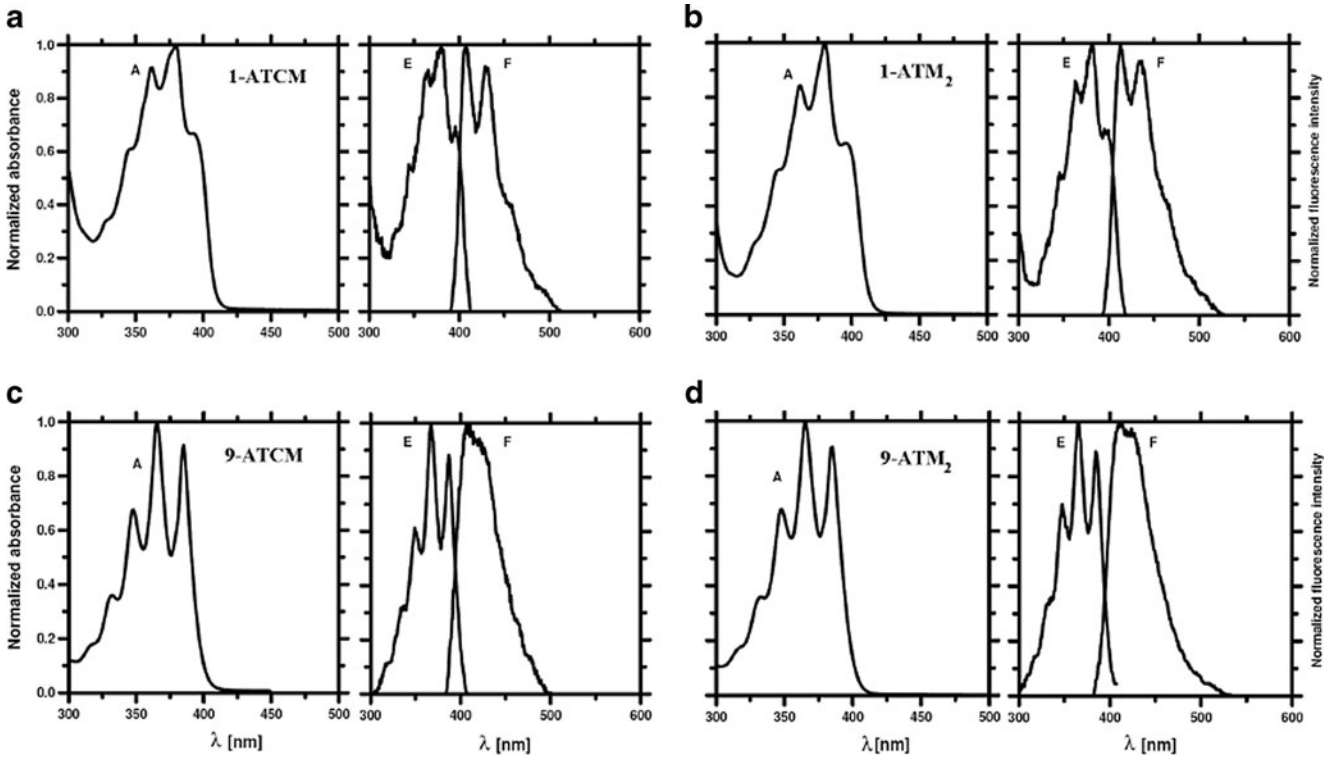

Fig. 3 Absorption (A), excitation (E) and fluorescence (F) spectra of **1-ATCM** (**a**), **1-ATM$_2$** (**b**), **9-ATCM** (**c**) and **9-ATM$_2$** (**d**) in dibutyl ether

Table 3 Fluorescence quantum yields of *N*-derivatives of studied aminoanthracenes

Solv.	1-AAc	1-ATC_2	1-ATCM	1-ATM_2	1-ATCAn	1-$ATAn_2$
DBE	0.26	–	0.22	0.27	0.28	0.48
EtAc	0.26	–	0.05	0.24	0.28	0.39
MeCN	0.24	–	–	0.26	0.12	0.37
	2-AAc[a]	2-ATC_2	2-ATCM	2-ATM_2	2-ATCAn	2-$ATAn_2$
DBE	0.65	–	0.25	0.39	0,35	0.41
EtAc	0.36	–	0.12	0.26	0,23	0.30
MeCN	0.39	–	0.03	0.37	0,18	0.43
	9-AAc	9-ATC_2	9-ATCM	9-ATM_2	9-ATCAn	9-$ATAn_2$
DBE	0.23	–	0.10	0.21	0.50	0.49
EtAc	0.19	–	0.03	0.16	0.21	0.26
MeCN	0.17	–	–	0.18	0.10	0.22

[a]see [9]

(DBE) to MeCN shifts the fluorescence maxima of **1-AA** bathochromically by 39 nm. The maxima of **9-AA** remained almost un-shifted. The Stokes shift for **9-AA** is very little dependent on the solvent polarity (94–101 nm); the considerably stronger solvent effect was found for **1-AA** (101 nm in DBE, 147 nm in MeCN).

The substitution of amino hydrogen with an electron-withdrawing substituent causes the strong hypsochromic shifts of fluorescence (about 70–115 nm). An influence of a substituent on triazinyl ring and of solvent polarity on the position of the fluorescence band of *N*-derivatives is small; nevertheless, some relationships between the fluorescence spectra, the solvent polarity and the molecular structures are apparent:

- with increasing solvent polarity, the fluorescence of the *N*-derivatives of both amines is bathochromically shifted only by several nm and also the Stokes shifts are small;
- with decreasing electronegativity of the triazinyl ring (with a successive substitution of chlorine atoms by methoxy or phenylamino groups), the bathochromic shifts of fluorescence were found for all *N*-triazinyl derivatives in used solvents; the strongest effect was observed by the substitution of both chlorine atoms with phenylamino groups.

Since the absorption maxima of all studied compounds are practically independent on the solvent polarity, the magnitude of Stokes shifts and their changes caused by solvent polarity are determined by the shifts of corresponding fluorescence maxima.

Fluorescence Quantum Yields

As in the case of 1-aminopyrene [7], 3-aminoperylene [8] and 2-aminoanthracene [9], the substitution of amino hydrogen atom of **1-AA** and **9-AA** by cyanuric chloride brings about total fluorescence quenching of corresponding compounds in all used solvents (Table 3). The substitution of one chlorine atom by electron-donating methoxy or especially phenylamino group causes a significant raising of q_F

Table 4 Fluorescence lifetimes [ns]

Compound	Ethyl acetate					Acetonitrile				
	A_1	τ_1[ns]	A_2	τ_2 [ns]	χ^2	A_1	τ_1 [ns]	A_2	τ_2 [ns]	χ^2
1-AAc	1	4.07	–	–	0.97	1	5.02	–	–	0.98
1-ATCM	0.52	0.96	0.48	0.49	0.78[a]	–	–	–	–	–
1-ATM2	1	3.80	–	–	0.94	1	5.36	–	–	0.96
1-ATCAn	1	2.80	–	–	1.17	1	1.43	–	–	1.25
1-ATAn2	1	6.15	–	–	1.06	1	7.47	–	–	1.08
2-ATM2	1	8.18	–	–	1.06	1	8.89	–	–	1.11
2-ATCAn	1	6.60	–	–	1.04	–	–	–	–	–
2-ATAn2	1	8.98	–	–	1.09	–	9.76	–	–	1.22
9-ATCM	1	0.70	–	–	1.79[a]	–	–	–	–	–
9-ATM2	0.53	2.92	0.47	1.37	1.03	0.69	2.95	0.31	1.08	1.13
9-ATCAn	0.63	3.60	0.37	1.39	0.99	0.44	1.75	0.56	0.85	0.83
9-ATAn2	0.06	3.14	0.94	2.85	1.10	0.81	2.53	0.19	1.46	1.09

[a]Quality of the fit is affected by low fluorescence quantum yield.

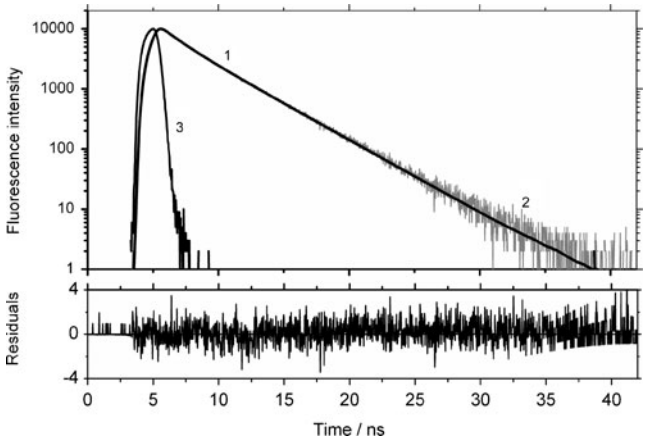

Fig. 4 Convolution of the Instrument Response Function (IRF, 3) with the two-exponential decay fit (1) to the 9-ATCAn fluorescence decay data (2) measured in ethyl acetate

of the corresponding derivatives in nonpolar DBE. With increasing solvent polarity, the q_F decreases; in high polar MeCN, the fluorescence is practically completely quenched for the chloromethoxy derivatives. The dimethoxy and phenylamino triazinyl derivatives exhibit relatively high q_F in used solvents. In contrast to *N*-triazinyl derivatives, *N*-acetyl derivatives of studied amines exhibit the relatively high q_F practically independently on solvent polarity.

Fluorescence Lifetimes

In all cases, the fluorescence lifetimes were observed to be sensitive to both the triazine ring substituent and the polarity of the solvent. The diphenylamino derivatives have longer fluorescence lifetimes than the dimethoxy derivatives; both compounds have longer lifetime in more polar MeCN than in less polar ethyl acetate (EtAc). The presence of one chlorine atom on the triazinyl ring and solvent polarity cause a decrease of the fluorescence lifetime of corresponding compounds.

As shown in Table 4, some of the triazinylated derivatives of aminoanthracene exhibit two-exponential fluorescence decay kinetics. An exaple of such decay curve and the corresponding fit is depicted in Fig. 4. Further studies aimed on resolving the origin of this phenomenon are currently in progress.

Theoretical Results

The equilibrium conformation of the studied molecules in their electronic ground state and the excited state

Table 5 Optimized geometry of the studied *N*-triazinyl compounds (γ ° corresponds to dihedral angle C1C2C4N5 the doted arrows denote the directions of anelation to form 1-, 2- and 9-anthracene derivatives)

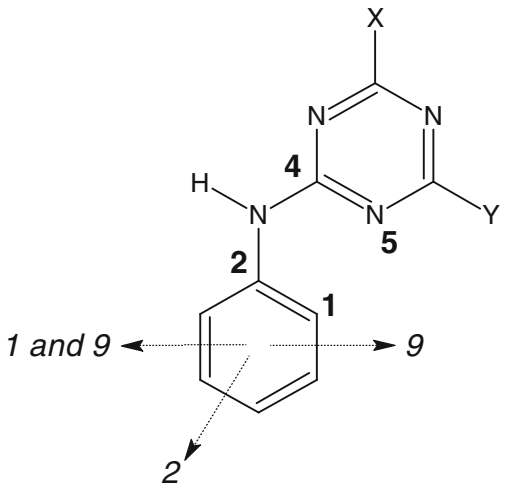

Compound	γ °	Compound	γ °
1-ATC$_2$	39	**2-ATAn$_2$**	33
1-ATM$_2$	40	**9-ATC$_2$**	53
1-ATAn$_2$	39	**9-ATM$_2$**	52
2-ATC$_2$	35	**9-ATAn$_2$**	52
2-ATM$_2$	34		

characteristics in vacuum and in DBE and MeCN were calculated using semi-empirical AM1 and ZINDO/CI methods respectively, implemented in ArgusLab 4.0 [16].

The optimized geometry of the *N*-triazinyl derivatives is presented in Table 5 (the computed theoretical values are rounded to integers). It is evident that the dihedral angle between the anthracenyl and triazinyl rings depends mainly on the position of the substitution on anthracene ring and not on the character of substituents on the triazinyl ring; a steric hindrance may play a role- the 9-derivatives exhibit the greatest dihedral angle.

The computed theoretical values are in Tables 6, 7, 8 rounded to integers (nm), to one decimal place (DM), to two decimal places (wave numbers and weights of main configurations) and to three decimal places (f).

The first two transitions of **1-AA** and **2-AA** are formed by the mixture of L_b and L_a transitions (Tables 6 and 7). The first transition of **9-AA** is of L_b type m→n+1, m-1→n, the second one is of HOMO-LUMO type m→n (Table 8). As in the case of *N*-acetyl and *N*-triazinyl derivatives of 1-aminopyrene [10], the first transition of the studied *N*-triazinyl derivatives of the selected aminoanthracenes corresponds to like L_b transition: a mixture of m→n+1, and m-1→n configurations for *N*-acetyl derivatives and a mixture of m-1→n and m→n+3 configurations for *N*-triazinyl derivatives; MO n+3 shows the same shape as MO n+1 for unsubstituted amines and the *N*-acetyl derivatives. The vacant MOs n+1 and n+2 of the *N*-triazinyl derivatives are completely localized on the triazinyl ring. The L_a transition is formed by m→n configuration for all *N*-derivatives of studied aminoanthracenes. Two new transitions appeared in the excited singlet states manifold for all *N*-triazinyl derivatives (Tables 6, 7, 8). These transitions are connected with a charge transfer (CT) from HOMO (m) localized on aminoanthracene to the MO's n+1 and n+2, localized on the triazinyl ring, respectively (Fig. 5). These transitions have a high dipole moment (DM). No mutual mixing among L_b, L_a and CT states was found for all studied *N*-derivatives of aminoanthracenes. However, there is a relatively strong mutual mixing of different CT configurations in CT states for all *N*-triazinyl derivatives except for *N*-derivatives of 9-

Table 6 ZINDO/S transitions of **1-AA** derivatives in vacuum

State	Energy (10^3 cm^{-1})/nm	Oscillator strength (f)	Main CI configurations	Dipole moment (DM)	Character of transition
1-AA					
1	27.93/358	0.056	m→n+1 (0.72) m-1→n (0.54) m→n (0.35)	2.1	Lb (La)
2	28.41/352	0.240	m→n (0.91) m→n+1 (0.30) m-1→n (0.20)	4.2	La (Lb) (397)
1-AAc					
1	28.16/355	0.031	m→n+1 (0.76) m-1→n (0.59)	4.6	Lb
2	28.83/347	0.289	m→n (0.95)	4.5	La (375)*
1-ATC_2					
1	28.58/350	0.022	m→n+3 (0.72) m-1→n (0.60)	4.3	Lb
2	29.12/343	0.321	m→n (0.96)	4.5	La (381)*
3	33.60/298	0.093	m→n+2 (0.89)	20.1	CT
4	35.27/284	0.005	m→n+1 (0.85)	22.9	CT
1-ATM_2					
1	28.55/350	0.023	m→n+3 (0.75) m-1→n (0.60)	2.3	Lb
2	29.15/343	0.304	m→n (0.96)	2.3	La (380)*
3	35.71/280	0.149	m→n+1 (0.81)	14.8	CT (mixed)
5	38.70/258	0.006	m→n+2 (0.64)	13.4	CT (mixed)

[a] Experimental value [nm] of the absorption maximum of the most intensive vibronic band in region 300–450 nm

Table 7 ZINDO/S transitions of **2-AA** derivatives in vacuum

State	Energy (10^3 cm^{-1})/nm	Oscillator strength (f)	Main CI configurations	Dipole moment (DM)	Character of transition
2-AA					
1	27.37/365	0.043	m→n+1 (0.62) m-1→n (0.54) m→n (0.50)	2.8	Lb (La) (396)
2	29.22/342	0.181	m→n (0.83) m→n+1 (0.39) m-1→n (0.33)	2.4	La (Lb) (335)
2-AAc					
1	27.89/359	0.018	m→n+1 (0.69) m-1→n (0.60)	4.4	Lb
2	29.27/342	0.206	m→n (0.92)	5.7	La (360)[a]
2-ATC_2					
1	28.36/353	0.021	m→n+3 (0.68) m-1→n (0.60)	3.9	Lb
2	29.53/339	0.190	m→n (0.93)	4.8	La (365)[a]
3	34.20/292	0.467	m→n+2 (0.81) m-1→n (0.32)	19.6	CT (mixed)
4	35.61/281	0.004	m→n+1 (0.78)	22.3	CT (mixed)
2-ATM_2					
1	28.26/354	0.025	m→n+3 (0.63) m-1→n (0.59)	1.8	Lb
2	29.59/338	0.193	m→n (0.91)	2.4	La (367)[a]
3	36.22/276	0.802	m→n+1 (0.73) m-1→n (0.38)	13.7	CT (mixed)
5	38.80/258	0.089	m→n+2 (0.57)	12.2	CT (mixed)

[a] Experimental value [nm] of the absorption maximum of the most intensive vibronic band in region 300–450 nm [9]

Table 8 ZINDO/S transitions of **9-AA** derivatives in vacuum

State	Energy (10^3 cm^{-1})/nm	Oscillator strength (f)	Main CI configurations	Dipole moment (DM)	Character of transition
9-AA					
1	27.24/367	0.073	m→n+1 (0.82) m-1→n (0.53)	1.9	Lb (410)
2	27.54/363	0.281	m→n (0.97)	2.1	La (375)[a]
9-AAc					
1	28.04/357	0.029	m→n+1 (0.78) m-1→n (0.60)	4.9	Lb
2	28.74/348	0.284	m→n (0.97)	4.9	La (367)[a]
9-ATC$_2$					
1	28.38/352	0.027	m→n+3 (0.76) m-1→n (0.60)	4.1	Lb
2	28.94/346	0.412	m→n (0.96)	4.5	La (366)[a]
3	32.45/308	0.007	m→n+2 (0.95)	21.9	CT
4	34.64/389	0.001	m→n+1 (0.95)	25.9	CT
9-ATM$_2$					
1	28.06/356	0.031	m→n+3 (0.76) m-1→n (0.59)	2.7	Lb
2	28.86/347	0.305	m→n (0.97)	2.4	La (365)[a]
3	34.60/289	0.012	m→n+1 (0.95)	18.6	CT
5	38.40/260	0.001	m→n+2 (0.88)	21.0	CT

[a] Experimental value [nm] of the absorption maximum of the most intensive vibronic band in region 300–450 nm

aminoanthracene. The high oscillator strength of the first CT transition (state 3) for *N*-triazinyl derivatives of **2-AA** is related to participation of locally excited (LE) anthracene m-1→n configuration. The shapes of MOs participating in discussed transitions are practically the same (9-*N*-derivatives) or are very similar to those of anthracene.

From the theoretical data it is evident that the excitation energies of the L_b and L_a transitions are mutually close and are only a little dependent on an *N*-substituent; it is in good agreement with the small shifts of experimental absorption maxima. But, regarding the strong overlap of the absorption bands, it is difficult to assign the theoretical transitions to the corresponding absorption L_b and L_a bands. The only exception is 2-AA where the both absorption bands are well separated [9] and the assignment of theoretical values is easier. In any case it is evident, that the ZINDO method predicts the excitation energy of the transitions too hypsochromically, especially for unsubstituted amines. Contrary to anthracene-type L_b and L_a states, the energy of the CT states raises with successive substitution of chlorine atoms by the methoxy or phenylamino group i.e. with a decrease of electronegativity of the triazinyl ring.

The calculations also show that the dependence of q_F of the studied compounds on their chemical structure and on the solvent polarity may consist in the presence of the CT states. Due to the high dipole moments of these states, their energy could fall in polar solvents to the vicinity or even below the fluorescent state and thus contribute to its non-radiative decay [10].

The ZINDO/S calculations taking into account the solvent, demonstrate the dramatic influence of solvent polarity on the energy of the CT states. We have calculated the singlet excited states energy of all *N*-derivatives for their optimized structure in DBE (f=0.096), and MeCN (f=0.305) (Fig. 6). According the expectations, the L_b and L_a states energy does not depend on solvent; their dipole moments slightly increase with increasing solvent polarity. On the contrary, the CT states of *N*-dichloro triazinyl derivatives show high dipole moments and their energy decreases in polar solvents approaching the L_a state. The largest drop of CT states energy was observed for the transition from vacuum to DBE; smaller differences were found between DBE and MeCN. The dimethoxy and diphenylamino compounds exhibit large L_a–CT gap, so the CT states cannot affect the mechanism of fluorescence quenching. The CT state energies for chloromethoxy and chlorophenylamino triazinyl derivatives are situated

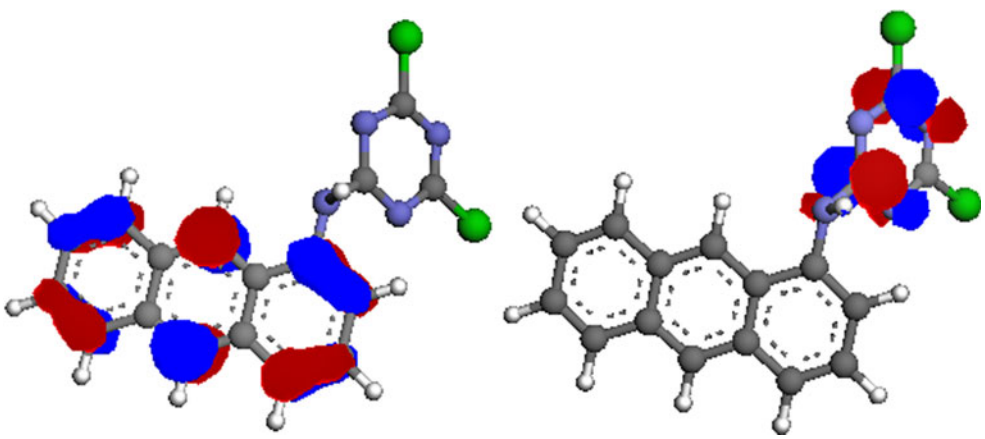

Fig. 5 The shape of HOMO (m) and vacant MO (n+2) for **1-ATC$_2$**

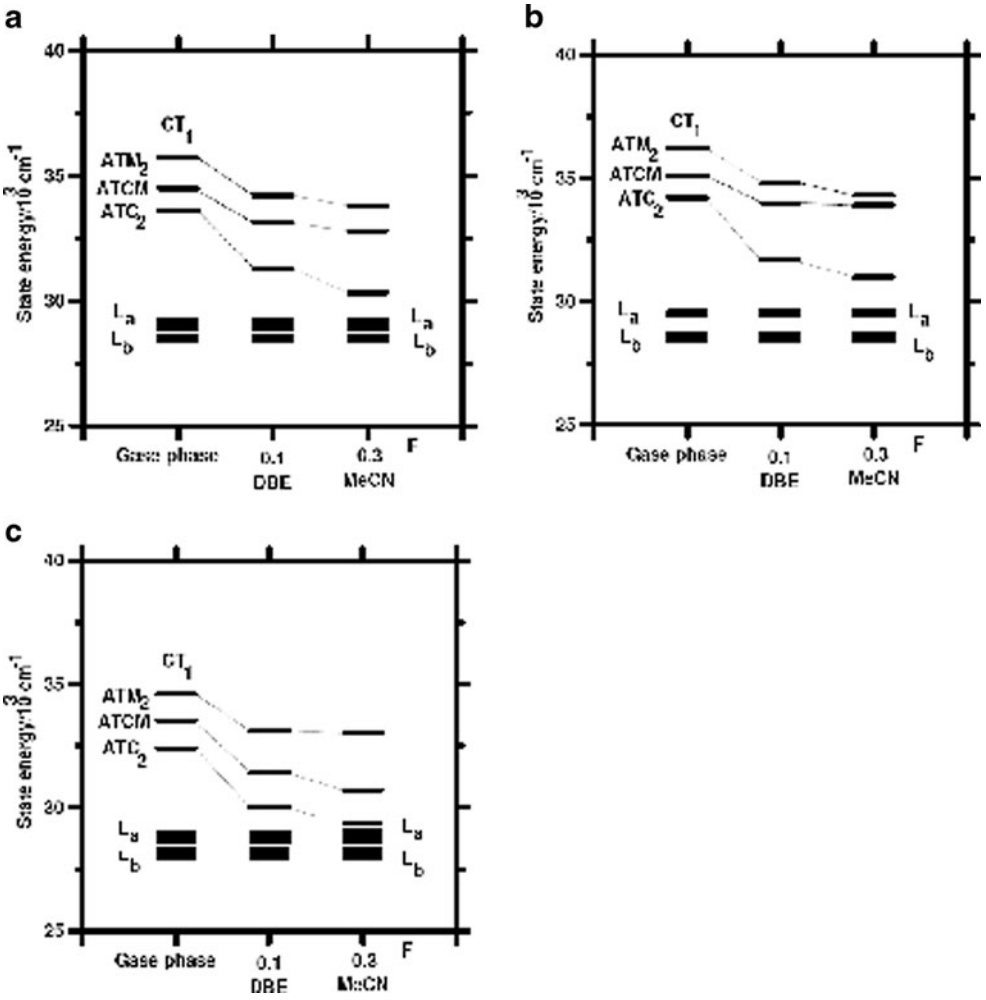

Fig. 6 ZINDO excited state energies in vacuum and in depending on solvent polarity function $F = (\varepsilon - 1/2\varepsilon + 1) - (n^2 - 1/2n^2 + 1)$, dielectric constant; n, refractive index of DBE and MeCN; **a**, **b** and **c** correspond to 1-amino, 2-amino and 9-amino antracenyl derivatives, respectively; the *thick lines* indicate the regions of the very close situated L_a and L_b states of the presented compounds

between the CT states of dichloro and dimethoxy or diphenylamino derivatives (Fig. 6). It corresponds well with the q_F of these compounds.

N-Acetyl derivatives show no CT states and, as expected, almost no dependence of their q_F on solvent polarity was found.

Conclusion

The series of new *N*-triazinyl derivatives of 1- and 9-aminoanthracenes was synthesized. Their chemical structure was confirmed by elemental analysis, MS and NMR spectra. The UV/Vis absorption and fluorescence spectra, fluorescence quantum yields and lifetimes were measured in several solvents of different polarity. The electronic character of substituents on the triazinyl ring and the solvent polarity mostly affect the position of the absorption and fluorescence maxima. As in the case of *N*-triazinyl derivatives of 1-aminopyrene, 3-aminoperylene and 2-aminoanthracene, the character of the substituents on triazinyl ring exhibit significant effect on q_F of the studied compounds: with increasing number of chlorine atoms on triazinyl ring (with its electron withdrawing character) and with increasing solvent polarity, the q_F of *N*-triazinyl derivatives of aromatic polynuclear amines is dramatically quenched.

The geometry and the electronic transition energies of the studied molecules were calculated using AM1 and ZINDO/S methods. It was found that besides the L_b and L_a $\pi\pi^*$ transitions localized on aminoanthracene moiety, there are transitions connected with strong charge transfer from HOMO localized on aminoanthracene to π^*MO localized on the triazinyl ring. These CT transitions show mostly low oscillator strength and a high transition dipole moment. Their energy decreases with increasing electronegativity of triazinyl ring (with increasing number of chlorine atoms) and dramatically with increasing solvent polarity. The same trends show the experimental fluorescence quantum yields. It is obvious that these CT states play an important role in excited state deactivation mechanism. The energy gap between the CT state and fluorescence emitting state energies is crucial for the fluorescence quantum yield of *N*-triazinyl derivatives of polynuclear aromatic amines.

References

1. Förster T (1965) In: Sinanoglu O (ed) Modern quantum chemistry, istanbul lectures, Part III. Academic, New York, pp 93–137
2. El-Sayed MA (1995) In: Molin TIY (ed) Ultrafast processes in chemistry and photobiology, a chemistry for 21st century monograph. IUPAC and Blackwell Science Ltd, UK
3. Khoo I-C, Simoni F, Umeton C (1997) Novel optical materials and applications. Wiley, New York
4. Fidler V et al (2002) Femtosecond fluorescence anisotropy kinetics as a signature of ultrafast electronic energy transfer in bichromophoric molecules. Z Phys Chem 216:589–603
5. Almonasy N et al (2009) Synthesis of bi- and trichromophoric dyes bearing ans-triazinyl ring spacer. Dyes Pigments 82:416–421
6. Kapusta P et al (2003) Photophysics of 3-substituted benzanthrones: substituent and solvent control of intersystem crossing. J Phys Chem A 107:9740–9746
7. Šoustek P et al (2008) The synthesis and fluorescence of N-substituted 1- and 2- aminopyrenes. Dyes Pigments 78(2):139–147
8. Almonasy N et al (2009) The synthesis of *N*-derivatives of 3-aminoperylene and their absorption and fluorescence properties. Dyes Pigments 82(2):164–170
9. El-Sedik et al (2012) Synthesis, absorption and fluorescence properties of *N*-triazinyl derivatives of 2-aminoanthracene. Dyes Pigments 92(3):1126–1131
10. Nepraš M et al (2012) Electronic structure, spectra and photophysical properties ofN-triazinylderivatives of1-aminopyrene. Semiempirical theoretical study. Dyes Pigments 92(3):1331–1336
11. Hirano K et al (2009) A modular synthesis of highly substituted imidazolium salts. Org Lett 11(4):1019–1022
12. Rigaudy J et al (1981) Studies of meso-aminoanthracenes. VIII. Methyl 10-amino-9-anthracenecarboxylate. Oxidation and diazotization. Bull Soc Chim Fr 5–6(2):223–230
13. Verma SM, Singh MD (1977) Structural elucidation with nuclear magnetic resonance spectroscopy. Diels-Alder adducts of 1-aminoanthracene and maleic anhydride: restricted rotation about the aryl C(1)-N bond and intrinsic asymmetry about the imide (Nsp2-Csp3) system. J Org Chem 42(23):3736–3740
14. Birks JB et al (1963) The relations between the fluorescence and absorption properties of organic molecules. Proc R Soc A 275:135–148
15. Bures F et al (2006) Novel nitrogen ligands based on imidazole derivatives and their application in asymmetric catalysis. Tetrahedron: Asymmetry 17(6):900–907
16. Thompson MA (2009) ArgusLab 4.0, Planaria Software LLC, Seattle, WA, http://www.arguslab.com. 29